CLUSTER ANISOTROPIES IN COLLOIDAL AGGREGATION IN THE PRESENCE OF GRAVITY

Agustín E. González
Instituto de Ciencias Físicas, Universidad Nacional Autónoma de México,
Apartado Postal 48-3, 62251 Cuernavaca, México

ABSTRACT

The colloidal aggregation problem coupled with the sedimentation experienced preferentially by the large clusters is stratified, the structural and dynamical quantities describing the aggregates depending on the depth at which they are measured. In this work we will use a new computer algorithm for colloidal aggregation coupled with sedimentation, that is capable of proportioning the average of these quantities inside a layer at a fixed depth and of arbitrary thickness in the aggregation prism. The dynamics, using this algorithm, will be shown to be in accordance with the experimental results. We have also found that (i) *in some cases* of sedimentation strengths and layer depths, the mean width (perpendicular to the gravitational field direction) and the mean height of the large settling clusters scale with the size as a power law, with the same scaling power, in some range of cluster sizes. This leads to self-similar clusters with an appreciably higher fractal dimension (d_f) than the d_f of aggregating clusters driven purely by diffusion (DLCA). However, (ii) there are some other cases for which the parallel and perpendicular scaling powers differ. (iii) There are still cases for which only the mean width *or* the mean height scale as a power law. Finally, (iv) there are further cases for which neither the mean width nor mean height scale as a power law with the size. In the last (ii), (iii) and (iv) cases the settling clusters are anisotropic and a fractal dimension cannot be defined by them.

1. INTRODUCTION

Particle aggregation is of great interest not only due to the variety of roles it plays in biological systems, medical diagnostics, paints and coatings, and numerous foods, but also as a model system for growth under non-equilibrium conditions. In the past two decades, work has focused on the formation of aggregates, including their geometry and growth kinetics, in the absence of sedimentation. After the proposal of a single-aggregate model by Witten and Sander [1], and more adequate for our purpose of colloidal aggregation, after the development of a diffusive model for cluster aggregation, simultaneously made by Meakin [2] and by Kolb *et al* [3], the number of works dealing with the aggregation of particles has increased considerably. However, many real aggregation phenomena rarely take place under quiescent conditions but instead occur in the presence of gravitational fields or macroscopic flows. In addition, external fields, including electrical, magnetic, and optical, have proven useful for assembling and moving colloidal particles, techniques that should be useful when dealing with particles of nanometers in size, since they are barely affected by gravity. Among the many examples for which the sedimentation effect is important we can cite the clearing or clarifying of liquids, the settling of bacteria clusters in quiet water, the aggregation and deposition of asphaltenes in crude oil, and a number of precipitation techniques employed by the chemical industry.

By adding salts or flocculants, which screen the electrostatic repulsion between the particles or which establish bridges between them, it is induced the aggregation of the particles into clusters, which themselves collide with other clusters, stick together and become larger. Initially, the aggregates are small and essentially move by diffusion. As the aggregation proceeds, the settling velocity of the large aggregates becomes significant, and a new mechanism for the movement of these large clusters appears. As the sedimentation velocity of the small aggregates is lower than that for the larger ones, these large clusters catch up with the smaller ones, actually sweeping them and becoming in the process larger and larger. As a result, the hitting rate between aggregates increases, which leads to an acceleration of the aggregation kinetics. However, as the colloidal matter in the bulk becomes more and more scarce, the aggregation kinetics eventually slows down. In the final state and for the non-gelling cases (low concentrations), the system is composed of a tenuous sediment on the bottom and a clear fluid above.

Experimentally, this new problem of aggregation coupled with sedimentation has been studied more extensively by Allain and collaborators [4, 5, 6], who found an increase in the fractal dimension (d_f) of the large, settling aggregates (reaching values as high as 2.2) [5, 6]. They attributed this increase in the d_f of the large clusters to a restructuring mechanism, due to the hydrodynamic stresses felt by their branches when they drift downwards. They also found the large settling aggregates to be non-rotating. This behavior was interpreted in Refs. [7, 8] in terms of a non-homogeneity of these clusters, being denser in their lower part, which is the one that is sweeping the smaller clusters that attach to them. The large clusters therefore

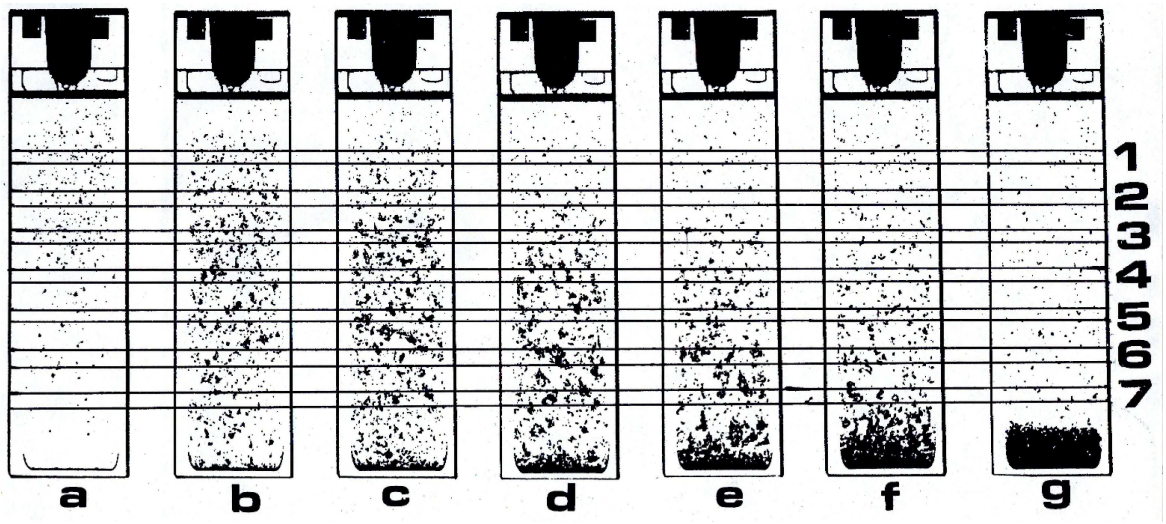

Figure 1: The states at different times of a Calcium Carbonate aggregating suspension of spherical particles, for the following times: (a) 5 min 20 s, (b) 6 min 20 s, (c) 6 min 40 s, (d) 7 min, (e) 7 min 20 s, (f) 7 min 40 s, (g) 8 min (from Ref. [4]).

act as badminton shuttlecocks that, when left rotating at a certain altitude, at the end they fall at constant velocity without rotation.

On the simulational side and in our first works [7, 8, 9] that consider both sedimentation and deposition (through a rarefaction of colloidal matter in the bulk), due to computational limitations, the structural (d_f) and dynamical quantities (basically the weight-average cluster size $S_w(t)$) were obtained from averages over the clusters inside the aggregating prism, independent of their vertical position. This assumption was necessary in order to have good statistics for the evaluation of the averages of highly fluctuating quantities. However, the colloidal aggregation problem coupled with sedimentation *is not* homogeneous on the vertical direction. In Fig. 1 we are reproducing figure 1 of Chapter III of Ref. [4] (the horizontal straight lines were added by the present author). In their system with a colloidal volume fraction of $\phi = 0.001$, the Calcium Carbonate spherical colloidal particles were of a diameter of 0.07 μm; therefore, they cannot be optically seen unaggregated, and even the smallest points shown in the confinement prism are actually clusters of many particles. The prism was illuminated from behind in such a way that what we actually see are the shadows of the clusters. We can clearly see in this figure that, for a sufficiently long time, the large clusters lie preferentially deeper than the smaller ones, which leads to a stratification of the system, as mentioned. Moreover, in each of the seven sublayers shown, we can also see that the average cluster size increases with time and peaks at a certain time, diminishing afterwards. The deeper the layer is, the longer the time it takes to peak and the higher the value at which it peaks.

More recently, in Ref. [10], the authors considered a two-dimensional lattice model for aggregation coupled with sedimentation; that is, they considered the z coordinate on the direction of the field and only one horizontal coordinate. They found that, for some cases of high sedimentation strengths and within some range of sizes, the mean width of the large settling clusters scaled as a power law with the cluster size while the mean height did not, leading to anisotropic clusters for which a fractal dimension could not be defined. To proceed further in this problem, what we actually need is an algorithm capable of proportioning the *average* aggregation quantities at a *fixed* depth in the prism, and consider a good number of cases of sedimentation strengths and layer depths. In Ref. [11] such an algorithm was presented in the form of a letter in which, by the nature of its size, it was not possible to show all the different cases of sedimentation strengths and depths, that lead to different behaviors in this problem. In this paper we consider a number of interesting cases of sedimentation strengths and depths, with such algorithm, presenting in more detail two of the cases.

To simulate such a system of diffusing, sedimenting and aggregating particles and clusters, one needs to know by which amount a cluster of N particles undergoes sedimentation as compared to the distance diffused, during a certain Monte Carlo time. Let us consider the sedimentation velocity v_s experienced by a cluster of N spherical particles of radius a and mass m_o:

$$v_s = \frac{m_o(1-\rho/\rho_o)gN}{f} = \frac{m_o(1-\rho/\rho_o)g}{k_B T} DN \quad , \qquad (1)$$

where ρ_o is the particles density, ρ is that of the suspension fluid, f is the cluster's friction coefficient, D $(= \frac{k_B\,T}{6\pi\eta R_g})$ is its diffusion coefficient, R_g is its radius of gyration, η is the solvent viscosity and T is the temperature. Let t_o be the time for which the cluster diffuses a particle diameter ($d = 2a$), that is, $t_o = 2a^2/3D$. During the same

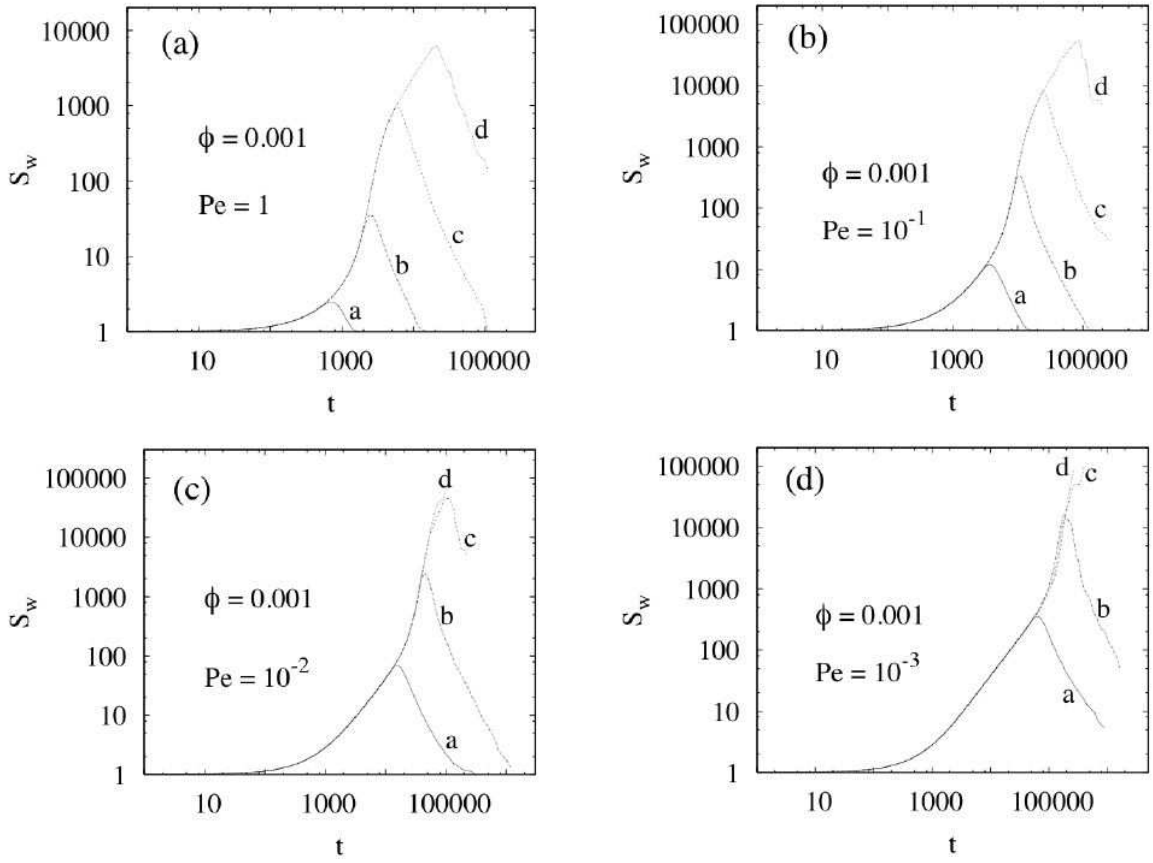

Figure 2: A log-log plot of the time evolution of the weight-average cluster size, S_w, for the Peclet numbers: (a) $P_e = 1$, (b) $P_e = 0.1$, (c) $P_e = 0.01$ and (d) $P_e = 0.001$. In all four figures the labels of each of the curves: a, b, c and d, correspond to the following depths: 500, 5000, 50000 and 500000, respectively.

time, the cluster drifts a distance $d_s = v_s t_o = \frac{1}{3} Pe\, Nd$, where $Pe \equiv m_o(1 - \rho/\rho_o)ga/k_BT$ is the Peclet number of the *individual* colloidal particles in the fluid. The Peclet number gives the sedimentation strength felt by the particles, being a number much smaller than one for most colloidal systems with a size generally smaller than $1\mu m$. It is in fact not difficult to show that if the colloidal particles are 1 μm in diameter, $1 - \rho/\rho_o$ is less than but of the order of unity, and T is room temperature, Pe is of the order of unity. However, if the diameter is 0.1 μm such quantity is of the order of 10^{-4}, while if the diameter is 10 μm, Pe goes as high as 10^4. Therefore, 1 μm marks the transition between diffusive and drifting behavior for *individual* particles, with density different from that of the medium.

The details of the algorithm are too long to be reproduced here. The interested reader is referred to Ref. [11] for those details. The volume fraction was fixed at the value $\phi = 0.001$. We considered 4 depths: $Z = 500, 5000, 50000$ and 500000, measured in terms of the diameter. For each of those depths, 5 Peclet numbers were considered: $Pe =$ 0.0001, 0.001, 0.01, 0.1 and 1.0 . In turn, for each Peclet number, a series of 10 simulations of 274625 particles were made in order to have enough statistics to evaluate the structural and dynamical quantities.

2. DYNAMICAL RESULTS

In Fig. 2 are shown the weight-average cluster sizes as a function of time, $S_w(t)$, for the Peclet numbers (a) 1.0, (b) 0.1, (c) 0.01 and (d) 0.001. As we can see in the figures, S_w increrases with time, peaks at a certain time and diminishes afterwards, a behavior that is in accordance to what we saw qualitatively in Fig. 1. We also note in all four figures that the deeper the layer we are considering, the longer the time it takes to peak and the higher the value at which it peaks, again in correspondance with Fig. 1.

3. STRUCTURE

The addition of a gravitational field on the vertical z direction in the colloidal aggregation problem, felt preferentially by the big clusters, introduces some degree of anisotropy in the structure of these clusters, as we will see below. It is therefore necessary to define and study some anisotropy measures of the clusters before trying to do a radius of gyration (R_g) *vs* size (N), log-log

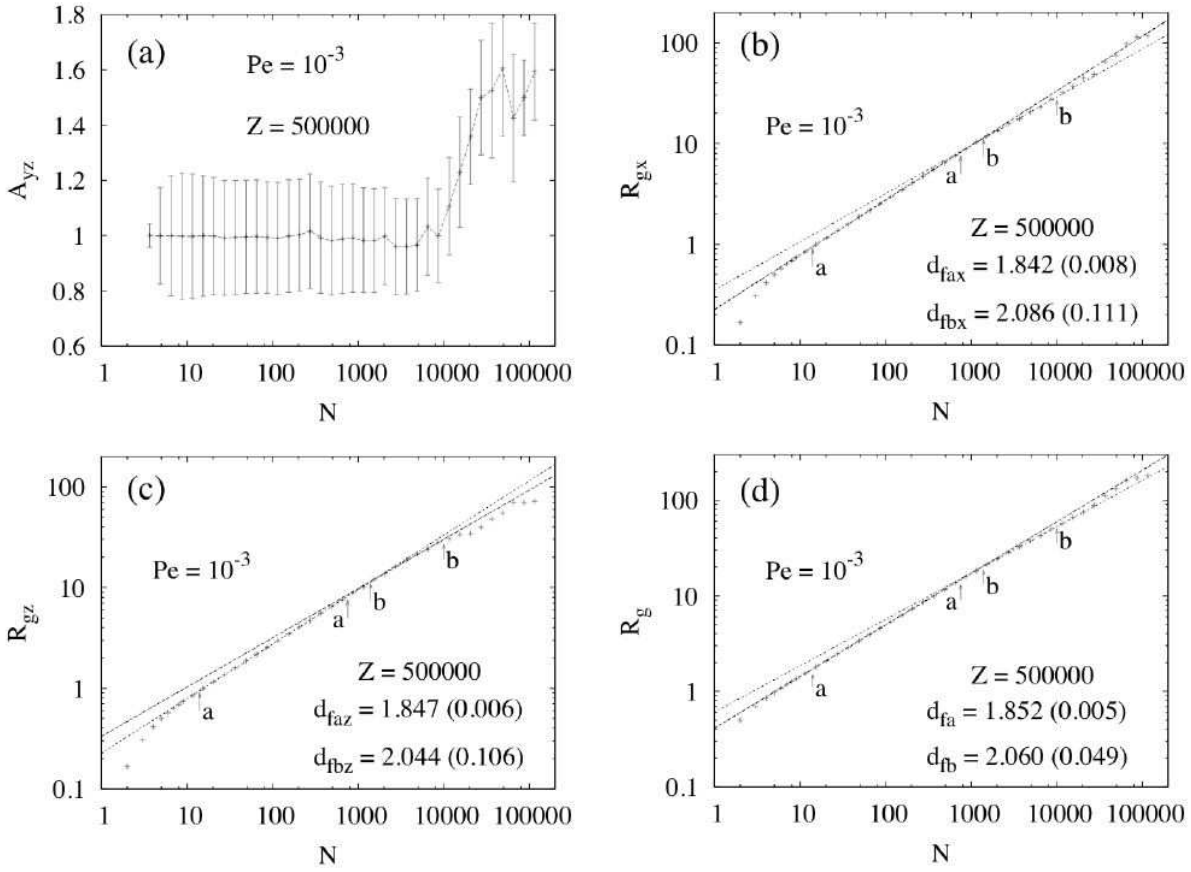

Figure 3: All four figures correspond to the layer at $Z = 500000$ and $Pe = 0.001$. (a) A plot of the anisotropy measure (see the text) A_{yz} *vs* the size. (b) A plot of R_{gx} *vs* the size. (c) A plot of R_{gz} *vs* the size. (d) A plot of R_g *vs* the size. In Figs. (b), (c) and (d) the plotted radii are averages over all clusters inside segments of constant magnitude in the logarithmic size scale N.

analysis, in order to see if it is possible to extract a fractal dimension from such plots. Let us define the anisotropy measures $A_{xz} \equiv < R_{gx}/R_g > / < R_{gz}/R_g >$ and $A_{yz} \equiv < R_{gy}/R_g > / < R_{gz}/R_g >$, where R_{gx}, R_{gy} and R_{gz} are the diagonal components of the radius of gyration tensor, such that $R_g^2 = R_{gx}^2 + R_{gy}^2 + R_{gz}^2$, and where the average values are calculated over all clusters inside segments of constant magnitude in the logarithmic size scale. Note that for isotropic clusters, the measures A_{xz} and A_{yz} should be equal to one, up to the statistical uncertainties. After studying the A_{xz} and A_{yz} quantities, we will make plots of not only $< R_g >$ *vs* N, but also of $< R_{gx} >$ *vs* N, $< R_{gy} >$ *vs* N and $< R_{gz} >$ *vs* N, to find any regions for which we have a power law scaling of those quantities. Here again the averages of the different radii are made over the same segments of constant magnitude in the logarithmic size scale. We have found a whole variety of behaviors for the structure of the clusters in this problem, depending on the sedimentation strength (Pe), the layer depth (Z) and the region of sizes considered. Generally speaking, the four radii (R_{gx}, R_{gy}, R_{gz} and R_g) scale as a power law with N, with the same scaling power, for the small, non-settling clusters, except for a number of cases with a high sedimentation strength: $Pe = 1.0$ for all depths and $Pe = 0.1$ for $Z = 500000$. In those cases of cluster isotropy it is therefore possible to define a cluster fractal dimension, This behavior shall be called the quasi-DLCA regime, where the "quasi" means that, as there is still some sweeping of even smaller clusters, the fractal dimension is a little bit higher than the usual DLCA d_f. For the large, settling clusters, we have found cases for which (i) the four radii again scale as a power law with N, with the same scaling power, making it possible to define a settling-clusters fractal dimension, a behavior that shall be called the sweeping scaling regime. There are however cases for which (ii) the scaling powers for the horizontal and vertical directions differ, obtaining therefore self-affine settling clusters. There are still some cases for which (iii) only the mean width *or* the mean height scale as a power law with N, and even further cases for which (iv) no scaling as a power law of the four radii is obtained.

3.1 The sweeping scaling regime

This regime is obtained at deep layers and intermediate

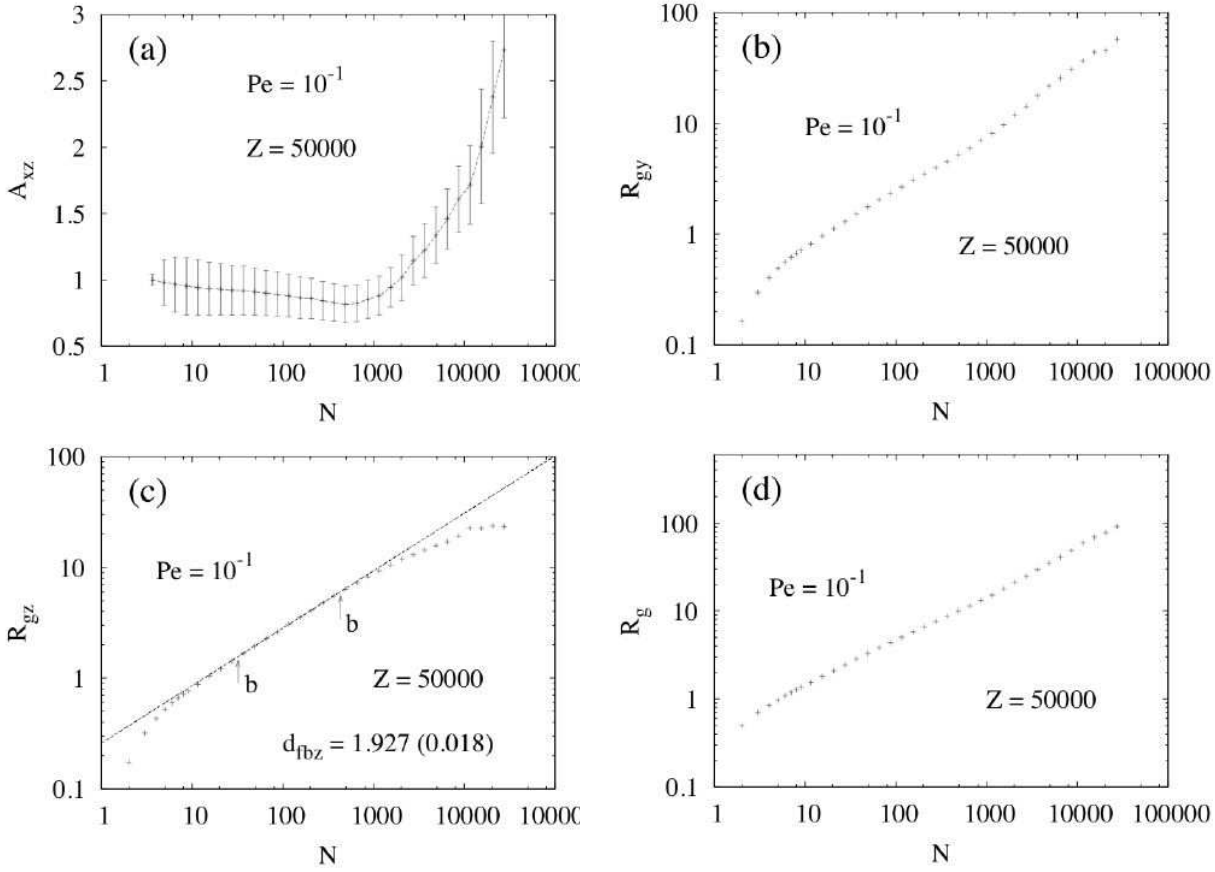

Figure 4: All four figures correspond to the layer at $Z = 50000$ and $Pe = 0.1$. (a) A plot of the anisotropy measure A_{xz} *vs* the size. (b) A plot of R_{gy} *vs* the size. (c) A plot of R_{gz} *vs* the size. (d) A plot of R_g *vs* the size.

Peclet numbers; the deeper the layer considered, the lower the Pe that can be used to attain the regime. In our studies we have found this regime for $Z = 500000$ with $Pe = 0.01, 0.001$ and 0.0001, and for $Z = 50000$ with $Pe = 0.001$. In Fig. 3 we are showing the case for $Z = 500000$ and $Pe = 0.001$. The anisotropy measure A_{yz} is first shown in Fig. 3a. As we can see, A_{yz} stays very close to one for all sizes up to about 10000, which is therefore the upper bound in this case for trying to obtain a fractal dimension from the log-log plots of the four radii *vs* N. After this upper bound, the clusters become definitely oblate. It should be mentioned that for the anisotropy measure A_{xz} we obtain a quite similar plot, with the same upper bound. In Fig. 3b is shown the log-log plot of the average radius R_{gx} *vs* N. After an initial curvature, correspondig to the corrections to scaling zone for small sizes, we obtain not one but two straight lines, before the upper bound is reached. This means that there are two zones for which we have scaling as a power law of the R_{gx} with N, one defined by the arrows labeled "a" and the other by the arrows labeled "b". The first one corresponds to the quasi-DLCA regime, with an inverse of the scaling power equal to $d_{fax} = 1.842 \pm 0.008$, while the second one has an inverse of the scaling power of $d_{fbx} = 2.086 \pm 0.111$. After the upper bound, the R_{gx} does not scale with N as a power law. For the average radius R_{gy} *vs* N a very similar plot is obtained, but this time with $d_{fay} = 1.851 \pm 0.010$ and $d_{fby} = 2.003 \pm 0.055$. The log-log plot of the average R_{gz} *vs* N is shown in Fig. 3c, where we can extract the following inverses of the scaling powers: $d_{faz} = 1.847 \pm 0.006$ and $d_{fbz} = 2.044 \pm 0.106$. Up to the statistical uncertainties, the scaling powers for the "a" zone coincide as well as those for the "b" zone. This means that it is therefore possible to obtain a fractal dimension for each zone. This is done in Fig. 3d, where we are plotting now the average R_g *vs* N. The inverses of the scaling powers provide us now with the following *fractal dimensions*: $d_{fa} = 1.852 \pm 0.005$, which corresponds to the quasi-DLCA regime, and $d_{fb} = 2.060 \pm 0.049$, corresponding to what we have called the "sweeping scaling regime" [8, 11].

3.2 Cases for scaling of the mean height or the mean width only

We have found cases for which the mean height scales as a power law with N while the mean width does not and viceversa. The cases of scaling of the mean height were for $P_e = 0.1$ with $Z = 50000$ and 5000, while those of scaling of the mean width were for $P_e = 0.01$ with

$Z = 50000$, and for $P_e = 0.1$ with $Z = 500$. In Fig. 4 we are showing the case $P_e = 0.1$ with $Z = 50000$. In Fig. 4a we can see that the anisotropy measure A_{xz} decreases very soon from one, reaching values around 0.8, which indicates somewhat elongated clusters. Afterwards it starts increasing very rapidly, crossing one and reaching values close to 3.0, which indicates this time very oblate clusters. A very similar plot was found for A_{yz}. In these cases of high $Pe's$, the quasi-DLCA regime disappears, hidden in the curvature of the zone of the corrections to scaling. However, for the settling clusters we can see that there is no scaling as a power law of the average R_{gy} *vs* size, as shown in Fig. 4b. The graph is all curved, with no possibility to define a straight line. A quite similar plot is obtained for the average R_{gx} *vs* size. Notwithstanding this, in Fig. 4c we can clearly see a zone of the settling clusters with a well defined straight line, which indicates scaling as a power law of the average R_{gz} *vs* N. The inverse of the scaling power was found as $d_{fbz} = 1.927 \pm 0.018$, above the DLCA fractal dimension. For the average of the whole R_g *vs* N we see again a curved graph, with no possibility to define a fractal dimension, as shown in Fig. 4d.

4. CONCLUSIONS

As it was seen, it is possible to devise an algorithm to study the colloidal aggregation problem coupled with sedimentation, that can provide us with the *average* aggregation quantities at a fixed depth in the aggregating prism. The higher value of the d_f for the sweeping scaling regime comes, in our case, from the sweeping of the small clusters by the large settling ones, which in turn occlude the holes and cavities of these large aggregates, increasing in this way their compacticity. Note that we cannot invoke a restructuring mechanism since it is not built-in in our model. Notice however that we have found a lower fractal dimension (~ 2.05) for the settling clusters than the one found by the experimentalists (~ 2.2) [6]. It is conceivable that also a restructuring of the large clusters would make them still more compact, helping to push its d_f up to about 2.2 . However, some other mechanisms could be present, like a sticking probabilitry lower than one (which would increase the d_f), the breakage of the clusters above a certain size (which may also increase their d_f), or the inclusion of the hydrodynamic interactions (whose effect on the d_f is unclear). As we have also seen, the present problem is richer than the colloidal aggregation problem driven purely by diffusion due to the whole variety of anisotropic cases obtained.

Acknowledgments

This work was supported in part by DGAPA-UNAM (PAPIIT Project IN118705-2).

References

[1] T. A. Witten and L. M. Sander, *Phys. Rev. Lett.* **47**, 1400 (1981).

[2] P. Meakin, *Phys. Rev. Lett.* **51**, 1119 (1983)

[3] M. Kolb, R. Botet, and R. Jullien, *Phys. Rev. Lett.* **51**, 1123 (1983)

[4] M. Wafra, *Ph. D. Thesis*, Université Paris-Nord, 1994

[5] C. Allain, M. Cloitre, and M. Wafra, *Phys. Rev. Lett.* **74**, 1478 (1995).

[6] C. Allain, M. Cloitre, and F. Parisse, *J. Colloid Interface Sci.* **178**, 411 (1996).

[7] A. E. González, *J. Phys. Condens. Matter* **14**, 2335 (2002).

[8] A. E. González, G. Odriozola, and R. Leone, *Eur. Phys. J. E* **13**, 165 (2004).

[9] A. E. González, *Phys. Rev. Lett.* **86**, 1243 (2001).

[10] M. Peltomäki, E. K. O. Hellén, and M. J. Alava, *J. Stat. Mech.* P09002 (2004).

[11] A. E. González, *Europhys. Lett.* **73**, 878 (2006).